Int. J. Electrochem. Sci., 12 **(2017)** 2135 – 2144, doi: 10.20964/2017.03.63

International Journal of
ELECTROCHEMICAL
SCIENCE
www.electrochemsci.org

Facile Synthesis of Fe_3O_4/graphene Nanosheets with High Conductivity for Application in Supercapacitors

Yan Wang[1], *Yibing Ma*[1], *Guizheng Guo*[1], *Yaya Zhou*[1], *Yinghe Zhang*[2], *Youyi Sun*[1,*], *Yaqing Liu*[1,*]

[1] Shanxi Province Key Laboratory of Functional Nanocomposites, North University of China, Taiyuan 030051, P.R.China.
[2] Nanotechnology Department, Helmholtz Association, 21502, Hamburg, Germany.
[*]E-mail: syyi@pku.edu.cn and lyqzgz2010@163.com

Received: 20 December 2016 / *Accepted:* 19 January 2017 / *Published:* 12 February 2017

The Fe_3O_4 grafted on monolayer graphene nanosheets (Fe_3O_4/GNs) were prepared by a facile method,. The structure and conductivity of Fe_3O_4/GNs were further characterized by X-ray diffraction, Transmission electron microscope, Atomic Force Microscope, Raman spectroscopy and four probe techniques. The results indicated that the Fe_3O_4 was uniformly coated on surface of monolayer GNs with high conductivity of 88.6S/cm. Moreover, the electrode based on Fe_3O_4/GNs has been characterized by the cyclic voltammetry, galvanostatic charge/discharge and electrochemical impedance spectra. The Fe_3O_4/GNs electrode exhibited excellent specific capacitance of 248.5 F/g, which was higher than that reported in previous works. The improvement was attributed to high conductivity and double-layer capacitance of the GNs. The work not only demonstrates the controlled synthesis of high-quality Fe_3O_4/GNs at mild conditions on a large scale, but also provides a universal route for the rational design of supercapacitors with high performance.

Keywords: monolayer graphene nanosheets; Fe_3O_4; liquid-phase exfoliation; electrical conductivity; supercapacitors.

1. INTRODUCTION

Fe_3O_4 as electrode materials of supercapacitors has attracted lots of attention due to its natural abundance, non-toxicity and low environmental impact [1]. However, its low conductivity and poor stability restricted its application in electrode materials of supercapacitors. To resolve these problems, a hybrid electrode material based on Fe_3O_4 and carbon materials with high conductivity has been investigated, such as graphite [2], carbon nanotubes [3-4] and graphene [5-14] . Especially,

combination of Fe_3O_4 nanoparticles with GNs was as an effective approach to achieve a superior electrochemical performance [10]. However, the reduced graphene oxide (rGO) was generally prepared from graphite oxide by heavy oxidation and chemical reduction in these works [5-14]. A great number of defects remained within the rGO, leading to be low electrical conductivity. So, in most cases, the Fe_3O_4/rGO were coated on the current collector with the addition of conductive materials (eg. acetylene black). Furthermore, the high resistance between Fe_3O_4/rGO and current collector would greatly decrease the capability of supercapacitors due to be low conductivity of Fe_3O_4/rGO. In addition to this, although the preparation of Fe_3O_4/rGO has been reported [5-14], but the preparation process was relative complexity, such as high temperature, low temperature, heavy oxidation and reduced treatment. These problems restricted practical application of Fe_3O_4/rGO in industry. So, it is still interesting to find a facile method of synthesis Fe_3O_4/graphene with high conductivity for application in energy storage.

Herein, a facile method of synthesis Fe_3O_4/GNs with high conductivity was reported, in which the GNs was prepared by the liquid-phase exfoliation method. The present method did not need low temperature, heavy oxidation and reduced treatment to attain the graphene. So, Fe_3O_4/GNs could be produced at high yield and in large quantities. Moreover, the GNs showed low defect concentration corresponding to high electrical conductivity and no reduction was needed at all, (ii) the GNs were low cost. These characteristics make the Fe_3O_4/GNs exhibited high specific capacitance, which is expected to apply in energy storage in the future.

2. EXPERIMENTAL

2.1Materials

Graphite intercalation compound (260ml/g, >99.5%) was supplied by the Qingdao Xinghe graphite company. $FeCl_3$ and $FeCl_2$ were supplied by the Shanxi Wanhua Cheminal Company, sodium hydroxide (NaOH) and acetone was purchased from Tianjin chemical Reagent company. All were analytical reagent.

2.2 Preparation of Fe_3O_4/GNs

The Fe_3O_4/GNs were prepared by three steps as shown in Scheme 1. Firstly, The GNs were synthesized by the liquid-phase exfoliation method. In brief, 0.5g graphite intercalation compound (GIC) was thermally shocked by the thermal treatment at 700℃ in a furnace to obtain the expanded graphite (EG). The EG was suspended in acetone under ultrasonication for 3.5h at 25℃, and then the GNs suspension acetone solution was obtained after removing the precipitate by centrifugation. Secondly, Fe_3O_4 magnetic fluid was prepared by co-precipitation method as shown in following: 3.58g $FeCl_2{\cdot}4H_2O$ and 6.08g $FeCl_3{\cdot}6H_2O$ were dissolved in 90mL distilled water to form a mixing solution. 92.4 ml NaOH aqueous solution (53mg/ml) was added into the mixing solution under vigorous stirring. The reaction continued for 90 min at 50℃. The Fe_3O_4 nanoparticles were separated with a

magnet.,They were washed for several times with deionized water and acetone to remove excess materials. Finally, the Fe_3O_4 nanoparticles were dispersed in acetone by ultrasonic for 30.0 min to forming Fe_3O_4 magnetic fluid with high stabilization. Thirdly, 30.0 ml Fe_3O_4 magnetic fluid (6.7mg/ml) was slowly added into the 60.0ml GNs solution (4.2mg/ml) at 80℃ under nitrogen flow with vigorous stirring. Then the Fe_3O_4/GNs were separated by external magnetic field and washed with acetone for several times. For a comparison, the Fe_3O_4/rGO was prepared by the modified Hummers method according to the previous works [5, 15].

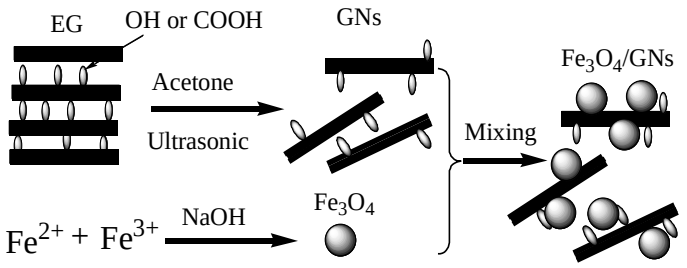

Scheme 1. The schematic diagram of the synthesis process of Fe_3O_4/GNs

2.3 Characterization

The morphology of GNs and Fe_3O_4/GNs were investigated by a transmission electron microscope (TEM, JEOL2100).

Raman spectrum of GNs and rGO was collected on a Jobin-Yvon Lab Ram HR800 Raman spectroscope equipped with a 514.5nm laser source.

The crystal structure of GNs and Fe_3O_4/GNs was characterized by X-ray diffraction on a Rigaku Dmax-r C X-ray diffractometer at 40.0kV and 100.0mA with Cu Kα radiation (λ =0.154nm).

AFM image of GNs was taken by a NTMDT NTEGRA SPM instrument with NSG03 noncontact 'golden' cantilevers.

Electrical conductivity of GNs and Fe_3O_4/GNs was measured by the the standard four probe techniques (using a Keithley 797A instrument).

2.4 Electrochemical performance

Electrochemical measurements, including cyclic voltammetry (CV), electrochemical impedance spectroscopy (EIS) (CHI 660D workstation) and galvanostatic charge/discharge curves (NEWARE BTS battery tester) were carried out in a three-electrode electrochemical cell using an Hg/HgCl (1M KCl filled) electrode as the reference electrode, a platinum wire as the counter electrode and the electrode materials (Fe_3O_4/GNs and polyvinylidene fluoride) supported Ni foam as the working electrode with 6.0 M KOH as the electrolyte. The mass ratio of Fe_3O_4/GNs and polyvinylidene fluoride (PVDF) was about 90:10. The Fe_3O_4/GNs loaded on each working electrode was about 5.0 mg. The specific capacitances were calculated by following equation:

$C = (I \cdot \Delta t)/ (m \cdot \Delta V)$

Where *C* is the specific capacitance (F/g), m is the mass of active material (g), ΔV is the applied potential window (V), *I* is the charge or discharge current, and Δ*t* is the time required for a full discharge.

3. RESULTS AND DISCUSSION

The preparation process of GNs was shown in Scheme 2. Firstly, the GIC was prepared by using acid and hydrogen peroxide as oxidant from graphite (G). Here, the oxidant should contain lots of -OH and -COOH groups , which was introduced to interlayer of graphite by the oxidant. It was benefited to reduce the Van der Waals' force of interlayer and enhanced the interlayer spacing of graphite. In addition, the oxidant did not destroy the sp^2 hybridized carbon of graphite , in which a little defects was formed within the graphite. Secondly, the EG was prepared by the thermal treatment of the GIC. In the process, the -OH and -COOH groups was removed by the high temperature treatment to form CO_2 and H_2O gas. Furthermore, the interlayer spacing of graphite increased due to expansive action of CO_2 and H_2O gas, resulting in reduction of Van der Waals' force within graphite. Thirdly, the EG was dispersed in solvent and was exfoliation by the expansive action of bubble from solvent under ultrasonication to form GNs [16]. Here, the solvent be introduction into interlayer of EG was key role, which was determined by the following two factors: (i) the interlayer spacing within EG is larger, and the solvent is easier introduction into interlayer of EG; (ii) the surface tension of solvent is litter, and the solvent is easier introduction into interlayer of EG. According to above discussion, the solvent acetone was choice to prepare monolayer GNs in present work.

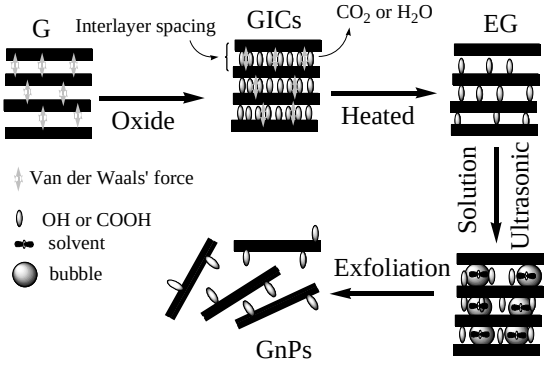

Scheme 2. The schematic diagram of the synthesis process of GNs

The formation of monolayer GNs was confirmed by the AFM image, TEM image and Raman spectra as shown in Fig.1A, Fig.1B and Fig.1C, respectively. As shown in Fig.1A, the products were sheet-like shape and the thickness of sheets was about 1.0nm. At the same time, it showed that the size of sheets was about hundreds of square nanometers. Fig.1B showed the TEM image of products. It clearly showed thin transparent layers and layered structure of GNs. The wrinkled morphology of the GNs was clearly visible in the image. Raman spectra of products prepared by liquid-phase exfoliation method were further characterized as shown in Fig.1C. It clearly showed three absorption peaks at

around 1340.0cm^{-1}, 1576.0cm^{-1} and 2686.0cm^{-1}, which were attributed to the D, G and 2D bands of graphene respectively[17]. D band related to the presence of substitutionally inplane heteroatoms, vacancies, grain boundaries or other defects, while G band referred to the quantity of ordered structures of the sp^2 hybridized carbon[17]. These results indicated the formation of monolayer GNs. It was well-known that the ratio of the D/G band intensity (I_D/I_G) represented the structural integrity of graphene and that the higher structural integrity showed the higher conductivity. The I_D/I_G was larger, and the structural integrity of graphene was lower. Here, the I_D/I_G (ca.0.11) of GNs was far lower than that (ca. 0.88) of rGO prepared by hummers method. So, the conductivity of GNs (221.6S/cm) was far higher than that of rGO reported in previous works.

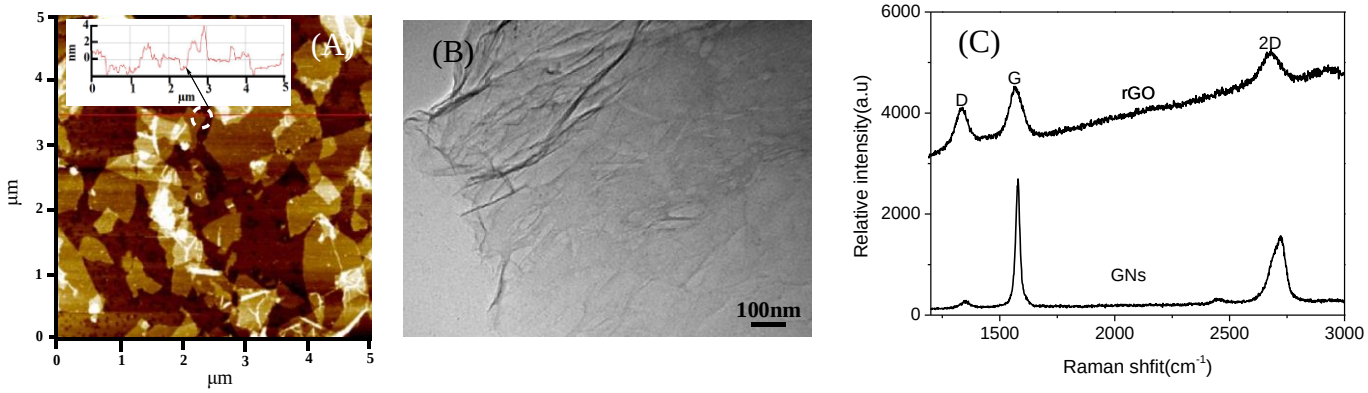

Figure 1. (A) AFM image, (B) TEM image, (C) Raman spectra of GNs and rGO.

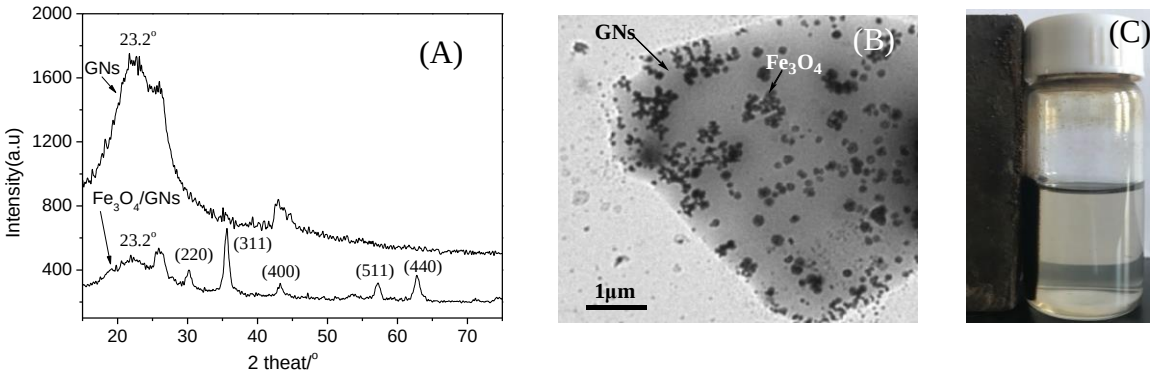

Figure 2. (A) XRD and (B) TEM image of Fe_3O_4/GNs, (C) is the photographs of Fe_3O_4/GNs in suspension solution under magnet.

The formation of Fe_3O_4/GNs was confirmed by the XRD and TEM image as shown in Fig.2A and Fig.2B, respectively. Fig.2A clearly showed some peaks at 30.5°, 36.0°, 43.6°, 57.8° and 63.0° for the Fe_3O_4/GNs, which were assigned to the (220), (311), (400), (511) and (440) lattice planes of cubic Fe_3O_4 (JCPDS card No. 88-0315), respectively [18]. In addition, excluding the diffraction peaks of Fe_3O_4, there was a diffraction peak at around 23.2°, which was ascribed to the (002) plane of GNs [19]. As shown in Fig. 2B, the nanoparticles were homogeneously distributed on the surface of the GNs.

The result indicated that the GNs effectively prevented the aggregation of Fe_3O_4 nanoparticles. When the Fe_3O_4 were dispersed into GNs suspension solution, the Fe_3O_4/GNs could be separated entirely from the suspension solution in 5s by an external magnet as shown in the Fig.2C. It is worth pointing out that neither the mechanical mixture of Fe_3O_4 particles nor GNs responds to an external magnet, and Fe_3O_4 particles will be separated from the suspension solution while the GNs will remain in suspension solution. It has been demonstrated that the Fe_3O_4 magnetic particles was adsorbed on surface of GNs [14]. These results confirmed the formation of Fe_3O_4/GNs.

Fig.3A showed the CV curves of GNs, Fe_3O_4/rGO and Fe_3O_4/GNs at 100.0mV s^{-1} within the potential range of 0~0.8V. For a comparison, the measured currents were normalized to the total mass of electroactive material. The CV curves of all samples exhibited nearly a rectangle shape, implying the perfect electrochemical capacitive behavior [20-21]. Furthermore, the CV area of the Fe_3O_4/GNs was much larger than that of the pure GNs and Fe_3O_4/rGO. It suggested that the specific capacitance of Fe_3O_4/GNs was larger than that of pure GNs and Fe_3O_4/rGO [22],.The CV curves of the Fe_3O_4/GNs as function of scan rate were characterized as shown in Fig.3B. The CV curve of Fe_3O_4/GNs was rectangular at 5.0mV s^{-1}, indicating a nearly ideal supercapacitor behavior. The peak current of CV curve increased with increasing in scan rate. In addition to this, the shape of CV curves showed some distortions from an ideal capacitor, possibly due to increasing over-potentials from ion transport between the eurveectrolyte and Fe_3O_4/GNs [23].

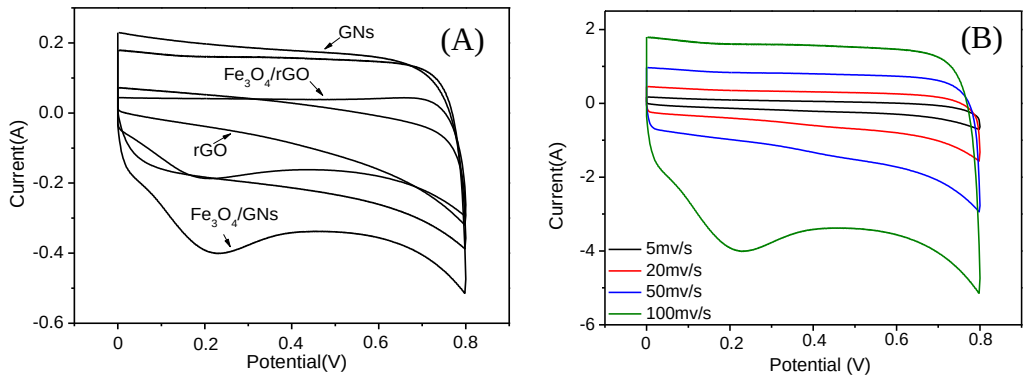

Figure 3. (A) the CV curves of GNs, rGO, Fe_3O_4/GNs and Fe_3O_4/rGO at 100mV s^{-1}, (B) the CV curves of Fe_3O_4/GNs at different scan rates.

The charge-discharge profiles of GNs, Fe_3O_4/rGO and Fe_3O_4/GNs were further compared as shown in Fig.4. The specific capacitance of the GNs, Fe_3O_4/rGO and Fe_3O_4/GNs were calculated from the galvanostatic-discharging curves and were shown in Table 1. Obviously, the specific capacitance (248.5F/g) of Fe_3O_4/GNs was higher than that (101.6F/g and 116.5F/g) of pure GNs and Fe_3O_4/rGO, suggesting an enhanced electrochemical performance of the Fe_3O_4/GNs. Furthermore, the Fe_3O_4/GNs still showed the highest specific capacitance comparing to Fe_3O_4/rGO reported in previous works. The result was firstly attributed to the synergistic effect of Fe_3O_4 and GNs [6]. The GNs could effectively prevent the aggregate of Fe_3O_4. At the same time, the Fe_3O_4 nanopartciles also could prevent the stack of GNs. So, the Fe_3O_4/GNs could offer a larger active surface area and more active sites to be accessed by electrolyte. Secondly, the GNs with high conductivity could effectively improve the conductivity of

electrode materials based on Fe_3O_4, which could build a highway for charge storage and continuous conductive paths for the transport of electrons. Thirdly, the GNs with monolayer were larger active surface area and more active sites.

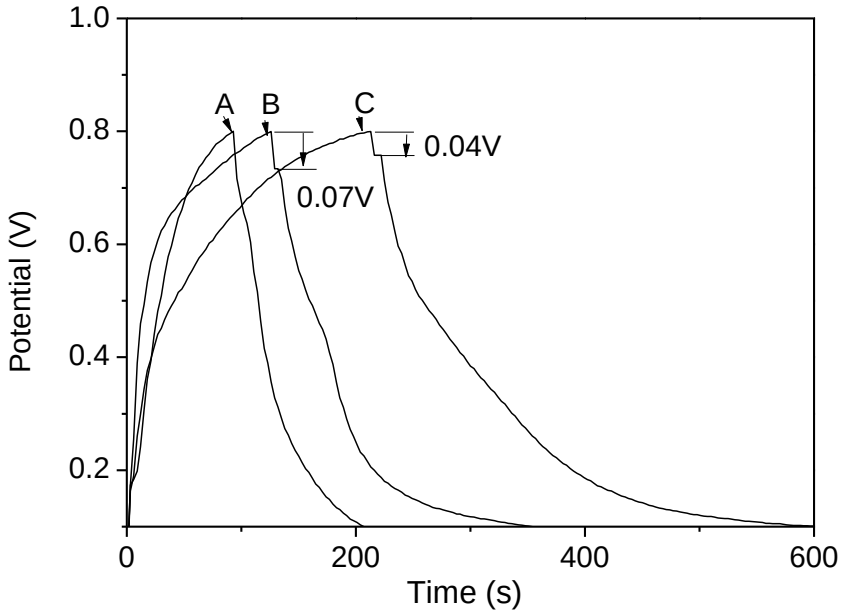

Figure 4. the charge and discharge performance of (A) GNs, (B) Fe_3O_4/GNs and Fe_3O_4/rGO at 2.5A/g.

Table 1. Properties of electrodes materials based on graphene and Fe_3O_4

Sample	Conductivity S/cm	Specific capacitance (F/g)	Current density A/g	Reference
GNs	221.6	101.6	2.5	Present work
Fe_3O_4/GNs	88.6	248.5	2.5	Present work
Fe_3O_4/rGO	0.4	116.5	2.5	Present work
Fe_3O_4/rGO		141.5	1.0	[6]
Fe_3O_4/rGO	-----	186.7	1.0	[7]
Fe_3O_4/rGO	----	195.0	1.0	[9]
Fe_3O_4/rGO	-----	212.0	1.0	[10]

The specific capacitance of Fe_3O_4/GNs as function of charge-discharge current densities and cycling number was also characterized as shown in Fig.5A and Fig.5B, respectively. It showed that the specific capacitances of Fe_3O_4/GNs was about 248.5F/g, 142.4F/g and 125.7F/g at a current density of 2.5A /g, 5.0A/g and 10.0A/g, respectively. When the current density increased from 2.5A /g to 10.0 A/g, the specific capacitance of the Fe_3O_4/GNs decreased from 248.5F/g to 125.7 F/g. The result

indicated that the Fe_3O_4/GNs had a relatively good rate capability. Fig.5B showed the cycling performance of the Fe_3O_4/GNs at 2.5A/g. The specific capacitance slightly decreased with increasing in cycling number. It was found that 98.2% of initial capacitance could be remained after 1000 cycles. The result indicated that the Fe_3O_4/GNs also exhibited a good cycling stability.

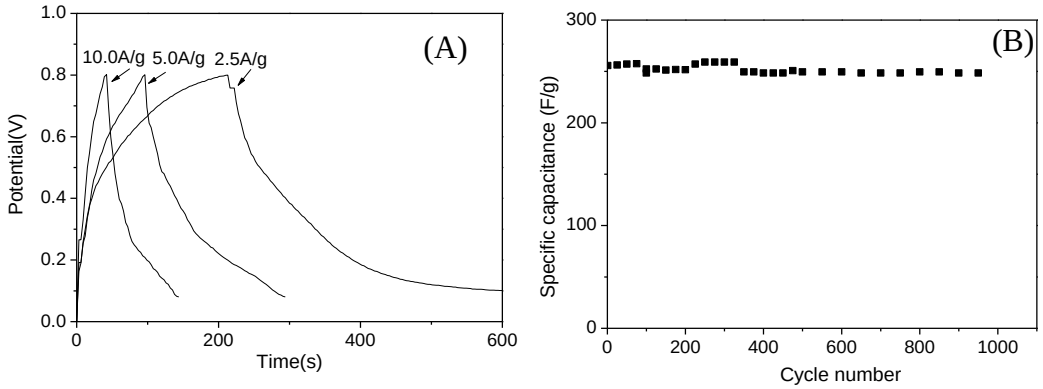

Figure 5. (A) Galvanostatic charge-discharge curves of Fe_3O_4/GNs at different current densities and (B) the specific capacitance of Fe_3O_4/GNs as function of cycling tests at a current density of 2.5A/g.

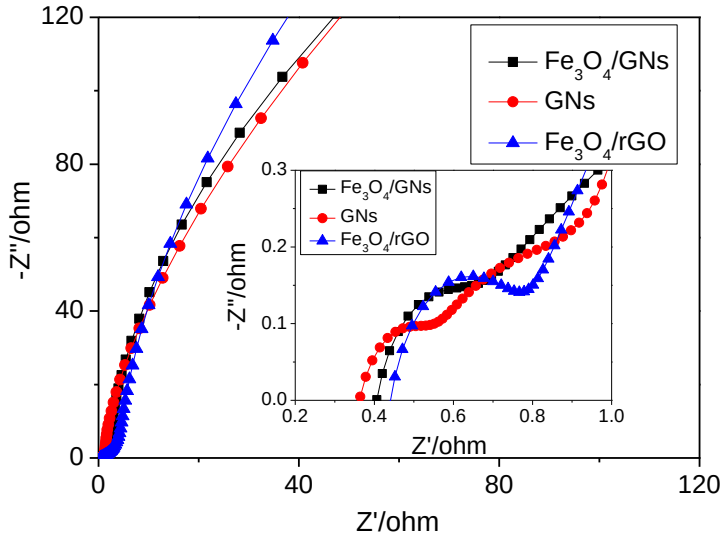

Figure 6. EIS curves of (A) GNs, (B) Fe_3O_4/GNs and (C) Fe_3O_4/rGO.

The EIS of GNs, Fe_3O_4/rGO and Fe_3O_4/GNs were also characterized and compared as shown in Fig.6. In the low-frequency region, the impedance plot increased sharply and tended to become vertical lines, indicating the characteristics of pure capacitive behavior [17]. At the high-frequency region, the intercept at real axis (*Z'*) represented the equivalent series resistance (ESR), which was attributed to ionic resistance of electrolyte, intrinsic resistance of substrate and contact resistance at the interface of active material/current collector[24]. At the same time, the semicircle represented the charge transfer

resistance (Rct) at the electrode/electrolyte interface. The ESR of GNs, Fe_3O_4/rGO and Fe_3O_4/GNs electrode was about 0.36 Ω, 0.44 Ω and 0.41 Ω, respectively. The result indicated that the intrinsic resistance and contact resistance of the Fe_3O_4/GNs was slight lower than that of Fe_3O_4/rGO, but higher than that of pure GNs. Additionally, the Rct of the GNs, Fe_3O_4/rGO and Fe_3O_4/GNs was about 0.13Ω, 0.23Ω, and 0.11Ω, respectively. The result indicated a shorter path for the ion diffusion for Fe_3O_4/GNs comparing to GNs and Fe_3O_4/rGO. Therefore, it could facilitate the efficient access of electrolyte ions to the Fe_3O_4/GNs and thus, would aid in delivering the high capacitance.

4. CONCLUSIONS

Monolayer graphene sheets (GNs) were prepared by a facile method, which might replace other carbon materials, such as carbon nanotube and graphite for fabricating electrodes with high electrical conductivity and barrier property for application in energy storage. Furthermore, the Fe_3O_4/GNs electrodes exhibited higher specific capacitance comparing to traditional electrode materials based on Fe_3O_4/rGO. The results were attributed to (i) increase in surface area and conductivity of the resultant composite due to the GNs with high conductivity and (ii) the major contribution of double-layer capacitance from the graphene and negligible capacitance from traditional electrodes materials.

ACKNOWLEDGEMENTS
The authors are grateful for the support by National Natural Science Foundation of China under grants (11202006), and the Shanxi provincial natural science foundation of China (2014021018-6).

References

1. S. Chandra, M. D. Patel, H. Lang and D.Bahadur, *J. Power. Sources.*, 280(2015)217.
2. D.F. Cao, N. F. Hu, *Biophys. Chem.*, 121**(**2006)209.
3. D.H.Guan, Z. Gao, W.L.Yang, J. Wang, Y. Yuan, B. Wang, M.L. Zhang and L.H. Liu, *Mat. Sci. Eng. B.*, 178(2013)736.
4. C.M. Chang, H.Y. Li, J.Y. Lai and Y.L. Liu, *RSC. Adv.*, 31(2013)12895.
5. S. Bhuvaneswari, P.M. Pratheeksha, S. Anandan, D.Rangappa, R.Gopalan and T.N. Rao, *Phys. Chem. Chem. Phys.*, 16 *(*2014) 5284.
6. T. Qi, J.J. Jiang, H.C. Chen and L. Zhang, *Electrochimica. Acta.*, 114 (2013) 674.
7. Q.H.Wang, L.F. Jiao, H.M. Du, Y.J. Wang and H.T. Yuan, *J. Power. Sources.*, 245 (2014) 101.
8. K.Wasinski, M.Walkowiak, P. Porolniczak and G. Lota, *J. Power. Sources.*,293 (2015) 42.
9. J.P. Cheng, Q.L. Shou, J.S. Wu, F. Lin, V.P. Dravid and X.B. Zhang, *J. Electroanal. Chem.*, 698 (2013) 1.
10. L. Li, Y.Y, Dou and L.F. Wang, *RSC. Adv.*, 4 (2014) 25658.
11. T.Z.Liu, X.D.Zhang, B.J. Li, J. Ding, Y.S. Liu, G. Li, X.H. Meng, Q. Cai and J.M. Zhang, *RSC. Adv.*, 4 (2014) 50765.
12. S. Saha, M.L. Jana, P. Samanta, N.C. Murmu, N.H. Kim, T. Kuila and J.H. Lee, *RSC. Adv.*, 4(2014) 44777.
13. Z.Y. Wang and C. J. Liu. *Nano. Energy.*, 11 (2015) 277.
14. B.J. Li, H.Q.Cao, J. Shao, M.Z. Qu and J.H. Warner, *J. Mater. Chem.*, 21 (2011) 5069.
15. Y.Y.Sun, W.H.Zhang, H.L. Yu and Y.Q. Liu, *J. Alloy Compd,* 638 (2015) 182.

16. Q.S. Meng, J. Jin, R.Y. Wang and C.H. Wang, *Nanotechnology.*, 25(2014) 125707.
17. Y.J.Zhang, H.J. Chi, W.H. Zhang, Y.Y. Sun, Q. Liang, Y. Gu and R.Y. Jing, *Nano-micro Lett.*, 6 (2014) 80.
18. Y.Y.Sun, Y.Tian, M.H. He, Q. Zhao, C. Chen, C.S. Hu and Y.Q. Liu, *J.Electron. Mater.*, 41 (2012) 519.
19. T.T. Liu, G.Z. Zhao , W.H.Zhang, H.J. Chi, C.L. Hou and Y.Y. Sun, *J. Porous. Mater.*, 22(2015) 1573.
20. Y.Y. Sun, W.H. Zhang, D.S. Li, L. Gao, C.L. Hou and Y.H. Zhang, *Electrochim. Acta.*,178 (2015) 823.
21. A.Allagui, T.Salameh and H.Alawadhi. *Inter. J. Energ. Res.*, 39 (2015) 1689.
22. C.Tran, D. Lawrence, F.W. Richey and V. Kalra, *Chem. Commun.*, 51 (2015) 13760.
23. S. Balasubramanian and P.K. Kamaraj. *Electrochim. Acta.*, 168 (2015) 50.
24. S.H. Kazemi, A. Asghari, and M.A. Kiani. *Electrochim. Acta.*, 138 (2014) 9.